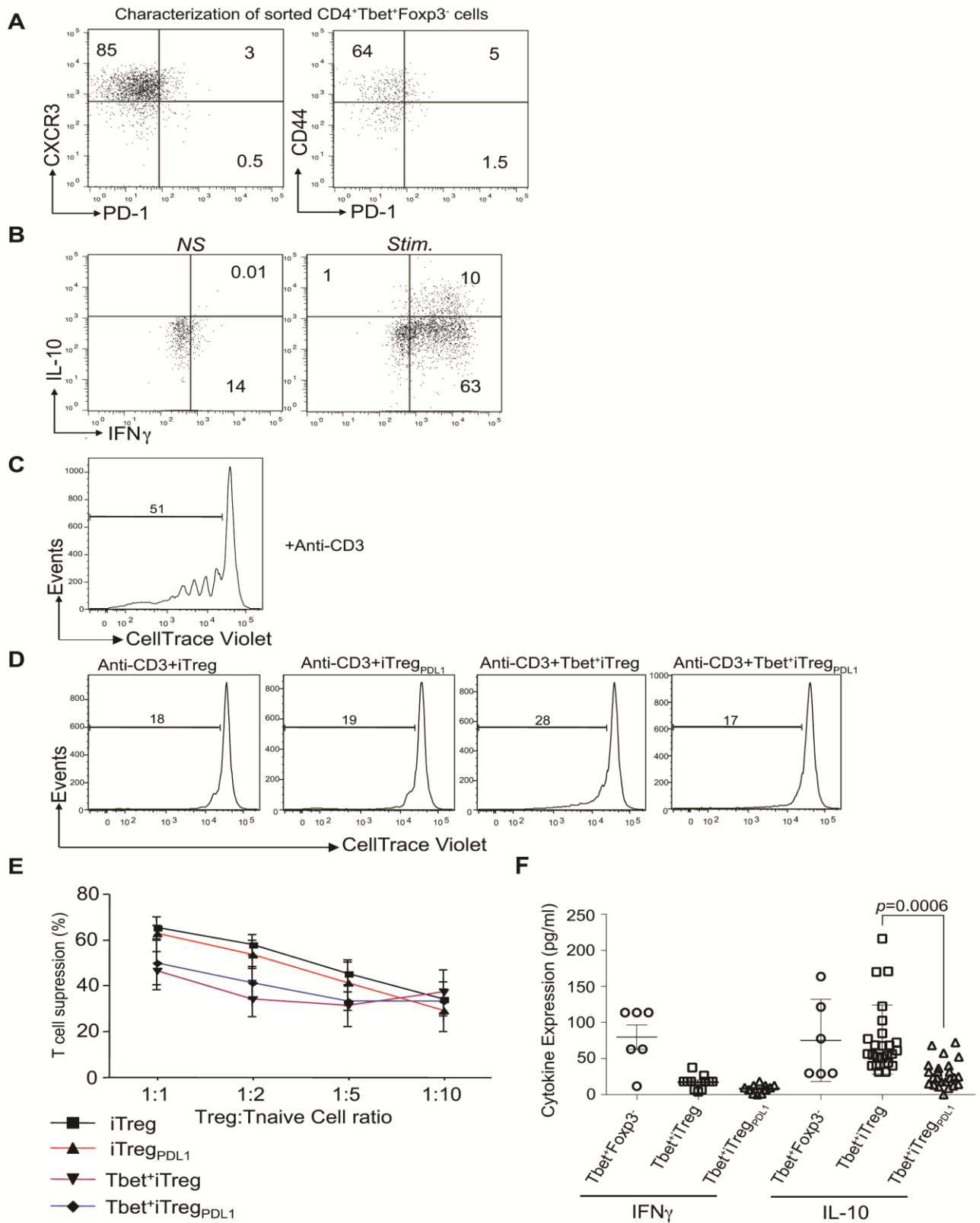


Supplementary Figure 1 (related to Figure 1)

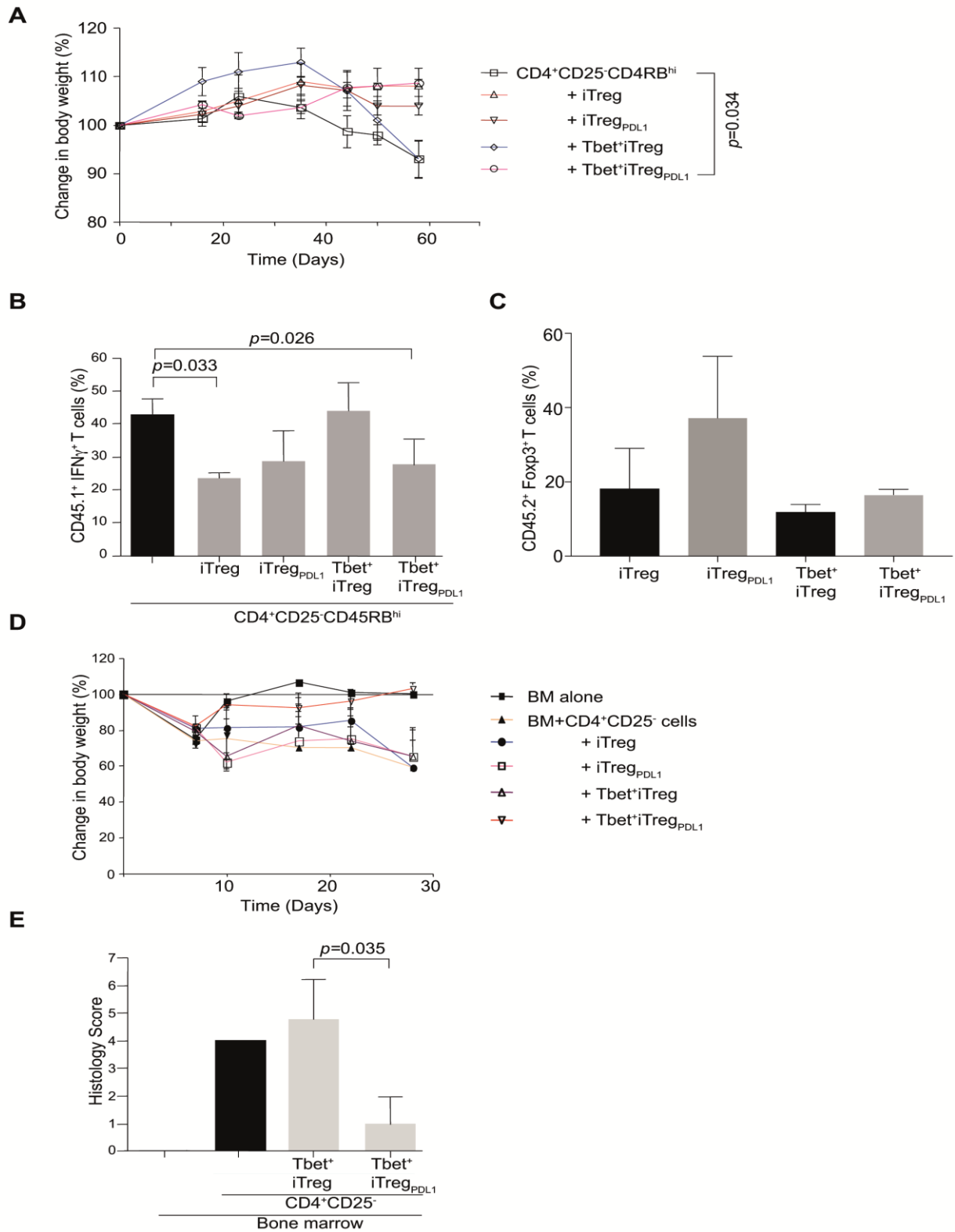


***In vitro* function of Tbet⁺iTreg cells and Tbet⁺iTreg_{PDL1} cells**

Characterization of flow sorted CD4⁺Tbet⁺Foxp3⁻ cells was performed prior to cell culture. Sorted cells had Th1 cell phenotype and expressed CXCR3, CD44 and PD-1 (A). Flow sorted cells also

expressed Th1 cytokines IFN- γ and IL-10, which was measured by intracellular flow cytometry (**B**). Tbet⁺ iTreg cells and Tbet⁺ iTreg^{PDL1} cells were generated from the flow sorted Tbet⁺ Foxp3⁻ cells and then utilized in an *in vitro* suppression assay. Responders were labeled with CellTrace Violet followed by stimulation with irradiated splenocytes and anti-CD3 and proliferation was measured by flow cytometry (**C**). Various Treg cell populations were added at different ratios and proliferation was measured (**D**). Summary data for three experiments was shown (**E**). Cytokine profile was obtained using Luminex from Tbet⁺ iTreg cells and Tbet⁺ iTreg^{PDL1} cells from at least 6 experiments (**F**). Experiments were repeated at least 5 times and each experiment was performed with n=3-5 mice and are presented as Mean \pm SEM.

Supplementary Figure 2 (related to Figure 2)

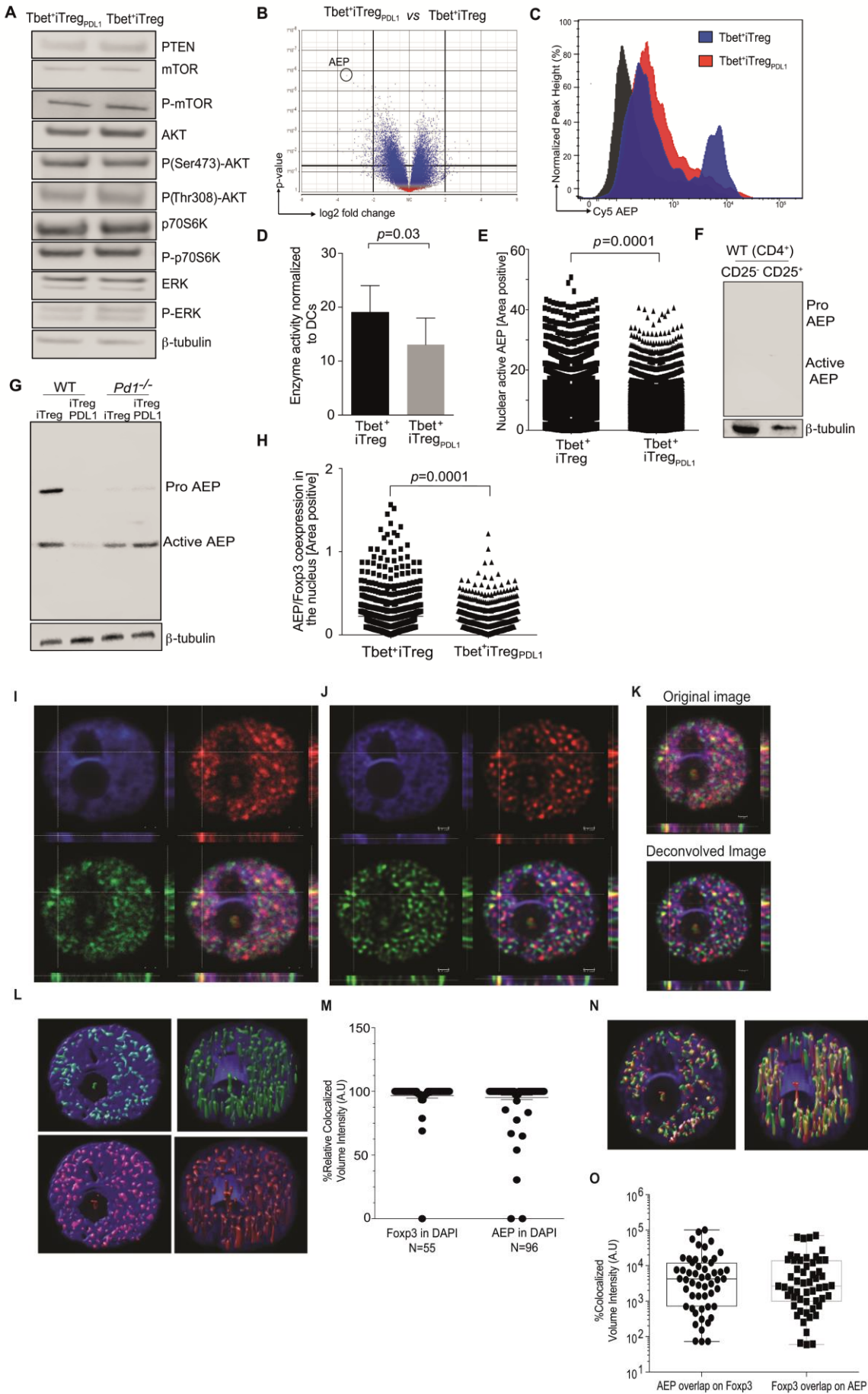


Tbet⁺iTreg_{PDL1} cells have regulatory function *in vivo*

Tbet⁺iTreg cells and Tbet⁺iTreg_{PDL1} cells were generated and then utilized for the prevention of autoimmune colitis and alloimmune GvHD. B6.Rag2^{-/-} mice were reconstituted with 4x10⁵

CD45.1⁺CD4⁺CD45RB^{hi}CD25⁻ T cells alone (T effectors) or along with CD45.2⁺ iTreg cells, iTreg^{PDL1} cells, Tbet⁺ iTreg cells and Tbet⁺ iTreg^{PDL1} cells (1x10⁵ cells/mouse). Weight loss was monitored in various cohorts (**A**). LPL were harvested for measuring immunological endpoints. Summary of T cell effector cytokine IFN- γ in various different cohorts was shown (**B**). Summary of Foxp3 (CD45.2⁺) expression in iTreg cells, iTreg^{PDL1} cells, Tbet⁺ iTreg cells and Tbet⁺ iTreg^{PDL1} cells in LPL (**C**). Function of Tbet⁺ iTreg cells and Tbet⁺ iTreg^{PDL1} cells were assessed in an experimental model of GvHD. Host Balb/c mice were subjected to lethal total body irradiation (950cGy) and then reconstituted with B6 T depleted bone marrow (BM) cells alone. All cohorts received CD4⁺CD25⁻ T cells in addition to BM. Certain cohorts received additional cell populations as indicated. Weight loss of mice that succumbed to GvHD over a period of 30 days in the various different cohorts (**D**). Histology of mice that received either Tbet⁺ iTreg cells and Tbet⁺ iTreg^{PDL1} cells was evaluated (**E**). For weight loss, each cohort consisted of n=10 mice. For histological, n=5 mice per cohorts were used. Cumulative data from 2 independent experiments are presented as Mean \pm SEM.

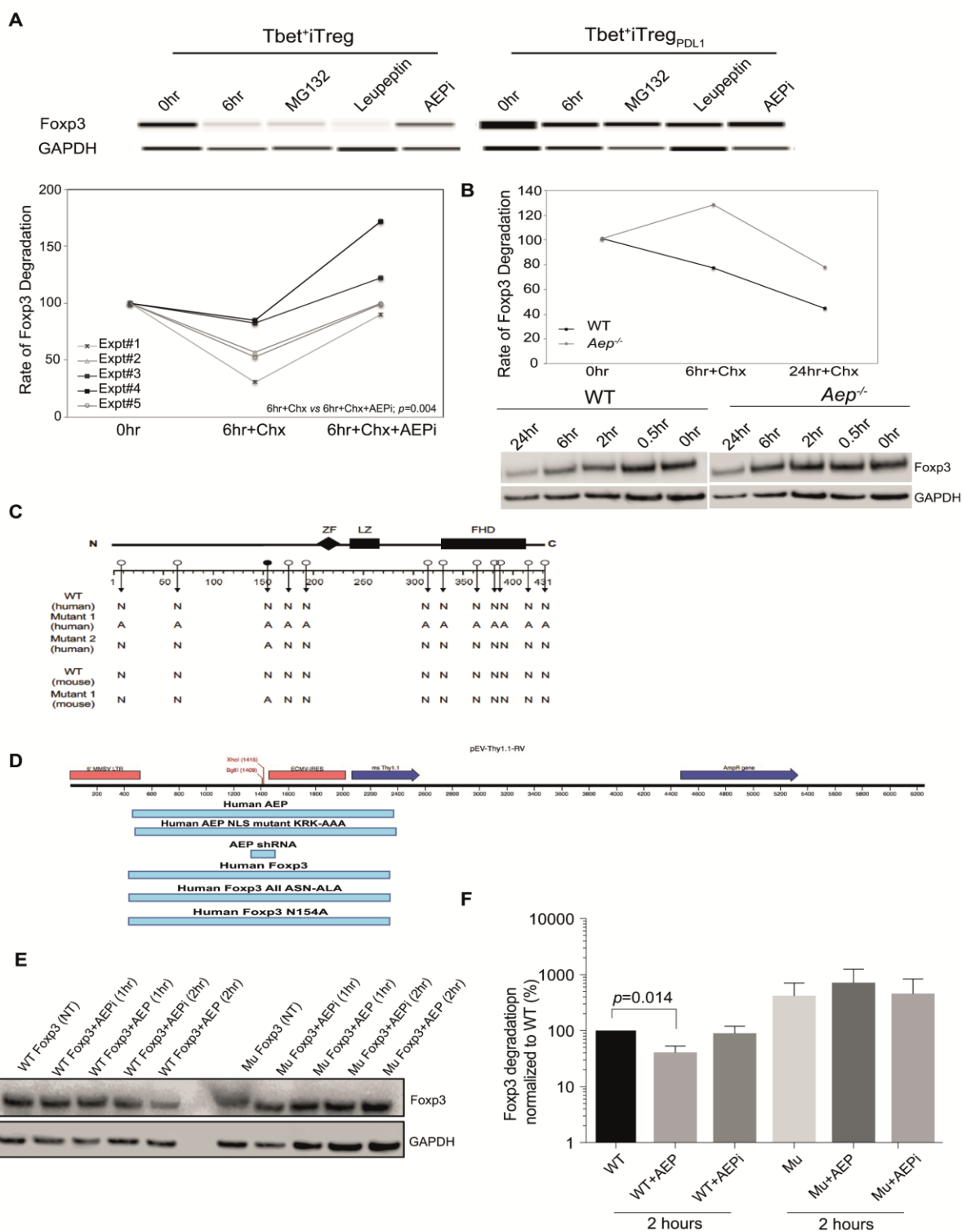
Supplementary Figure 3 (related to Figure 3)



PD-1 signaling downregulates AEP on Tbet⁺ iTreg_{PDL1} cells and iTreg_{PDL1} cells

Tbet⁺iTreg cells and Tbet⁺ iTreg_{PDL1} cell lysates were subjected to immuno blotting analysis to measure AKT and mTOR signaling pathway proteins (A). Volcano plot showing log₂ fold change versus p value in gene expression between Tbet⁺iTreg cells and Tbet⁺iTreg_{PDL1} cells (B). Expression of active AEP in Tbet⁺iTreg cells and Tbet⁺ iTreg_{PDL1} cells was measured by flow cytometry using the LE28 AEP Cy5 probe (C). AEP enzyme activity in Tbet⁺iTreg cells and Tbet⁺iTreg_{PDL1} cells (D). Summary plot showing AEP nuclear activity in Tbet⁺iTreg cells and Tbet⁺iTreg_{PDL1} cells (E). Naïve CD4⁺CD25⁻ T cells and CD4⁺CD25⁺ T cells were isolated from WT mice and lysates were tested for AEP by immuno blotting (F). Splenocytes were harvested from WT and *Pdl1*^{-/-} mice, and then naïve cells were isolated, differentiated under iTreg conditions alone or in the presence of PDL-1 fc. AEP expression was analyzed in *in vitro* induced WT and *Pdl1*^{-/-} iTreg cells (G). Summary plot showing AEP nuclear co-expression with Foxp3 in Tbet⁺iTreg cells and Tbet⁺iTreg_{PDL1} cells (H). Orthogonal projection view on confocal imaging data is shown in iTreg cells (I). The nucleus stained with DAPI and is depicted as blue, active AEP stained with activity probe AEP Cy5 is depicted as red and Foxp3 stained with Foxp3 PE is depicted as green. A quadrant is drawn on a particular point in the nucleus (blue image; top left panel) and then pasted on to AEP (top right panel) and Foxp3 staining (bottom left panel). If all three fluorophores are present together in this 3D view, then the analysis shows this on merging the three images (denoted as yellow in bottom right panel). The yellow is surrounded by blue in the x, y and z axis further suggesting the presence of active AEP and Foxp3 within the nucleus. Orthogonal projection view on deconvolved images (J). Deconvolution will correct optical aberration and provide higher resolution which enhances signal to noise ratio therefore minimizing false positive analysis. Combining deconvolution and orthogonal projection enhances our understanding of the spatial location and co-localization of proteins within a cell. Images processed by orthogonal projection and deconvolving is depicted on the top and bottom panels (K). Particle analysis of Foxp3 (L; top panels) and AEP (L; bottom panels) within the nucleus (L; left panels showing image of the cell at normal view and right panels at 60⁰) and quantitative analysis (M) is shown. Similarly, colocalization of AEP and Foxp3 within the nucleus is depicted (N; left panel and 60⁰ view right panel) and quantitative analysis (O) is shown. Experiments were repeated 3 times and representative immuno blots are shown. Cumulative data are shown as Mean±SEM.

Supplementary Figure 4 (related to Figure 3)

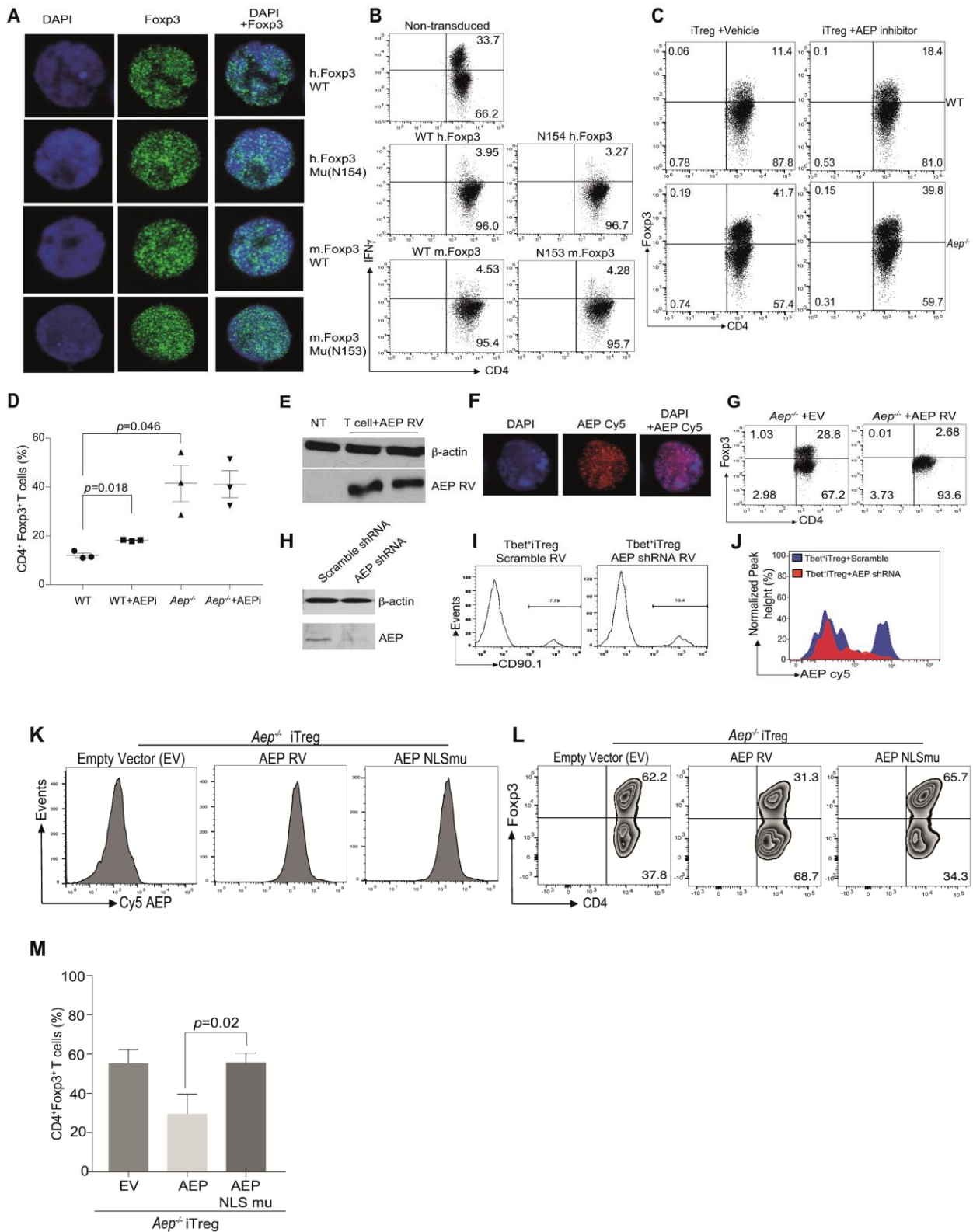


AEP inhibition prevents Foxp3 protein turnover in Tbet⁺iTreg cells and iTreg cells

Protein turnover was measured using standardized cycloheximide assays. Tbet⁺iTreg cells and Tbet⁺iTreg_{PDL1} cells were tested for the rate of Foxp3 turnover. Tbet⁺iTreg cells and Tbet⁺iTreg_{PDL1} cells were differentiated and then treated with cycloheximide (150μg/ml) at different time points. Certain conditions were supplemented with AEP inhibitor (AEPi; MV026630; 100 μM), or leupeptin (1mM)

or MG132 (0.5 μ M). Cell lysates were then subjected to immunoblotting (**top panel**). Foxp3 was normalized to the internal control GAPDH, and time 0hr was set as 100% then percent Foxp3 degraded is shown (**bottom panel**). Data is shown from 5 independent experiments (**A**). WT and *Aep*^{-/-} CD4⁺CD25⁻ T cells were differentiated under iTreg conditions and then Foxp3 turnover was measured in the presence of cycloheximide (**B**). Map showing AEP specific sites within the Foxp3 protein. The symbol N denotes Asparagine and A denotes alanine. Human mutant 1 was mutated at all N sites with A; human mutant 2 was mutated at N154 to alanine. Mouse mutant 1 was mutated at N153 to alanine (**C**). Plasmid map and the cloning sites of the various WT and mutant Foxp3, AEP shRNA, human AEP protein and mutant AEP protein were shown (**D**). Immuno blot of HEK293T cells transduced with human WT and mutant 1 human Foxp3. Cell lysates were subjected to AEP degradation assay and then WT and mutant human Foxp3 was determined (**E**). Relative amounts of WT versus mutant Foxp3 protein normalized to 0 hr WT and 0 hr mutant were shown (**F**). Experiments were repeated 3 times and data shown are from one independent experiment. Summary plots are depicted as Mean \pm SEM.

Supplementary Figure 5 (related to Figure 4)

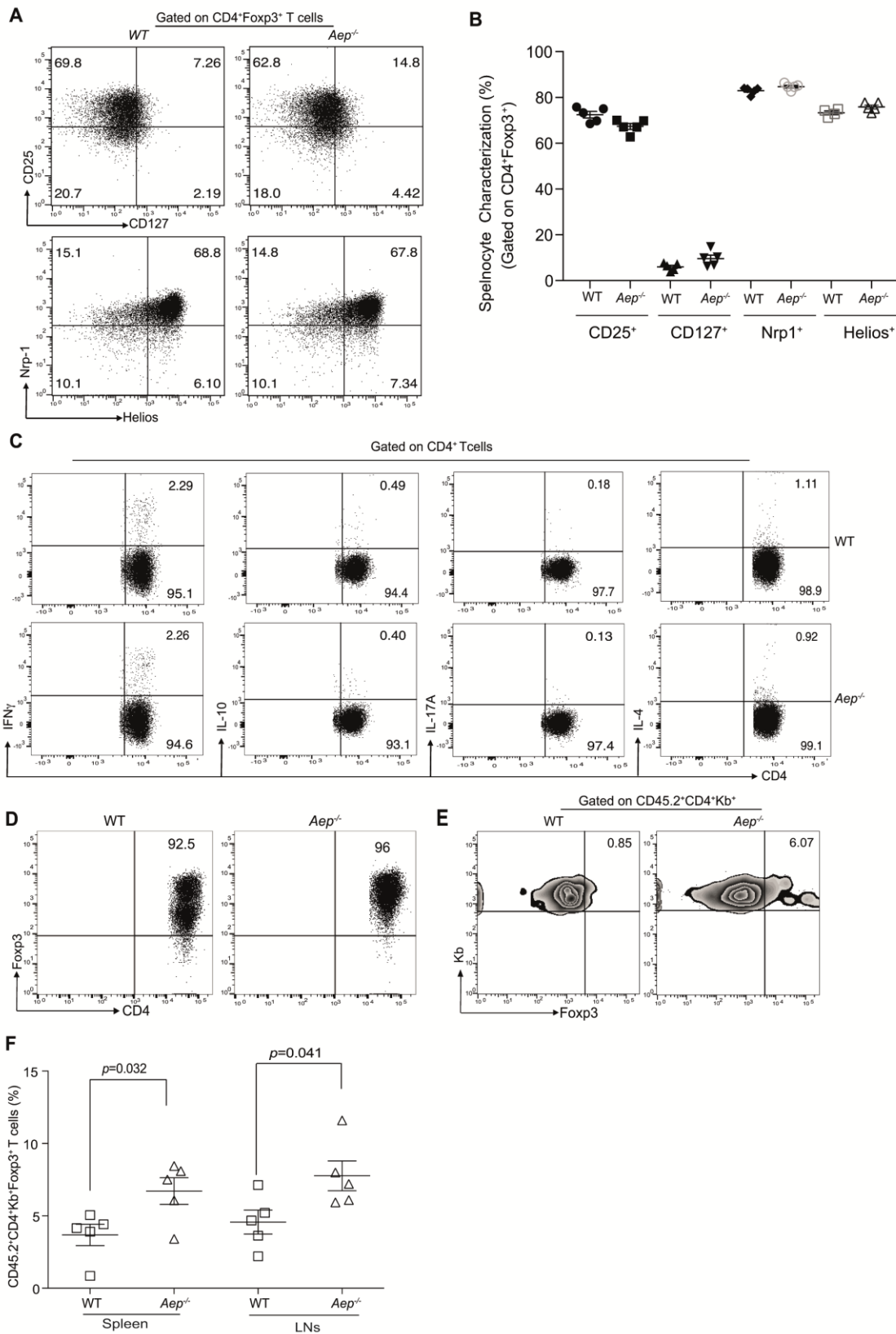


AEP specific Foxp3 mutation or AEP downregulation or AEP NLS mutation regulates Foxp3 protein stability.

CD4⁺CD25⁻ T cells from WT mice were activated with anti-CD3, anti-CD28 and IL-2 for 24 hrs and then transduced with human WT or mutant 2 human Foxp3 or mouse WT or mutant 1 mFoxp3. At day 4, cells were stained with DAPI and either human or mouse Foxp3 and then subjected to confocal microscopy (A). The ability of Foxp3 transduced cells to produce IFN-γ was tested by stimulating

the cells with PMA plus ionomycin for 4 hrs and golgistop and golgiplug were included during the last 2hrs of stimulation. Cells were then subjected to intracellular flow cytometry (**B**). CD4⁺CD25⁻ cells were isolated from WT and *Aep*^{-/-} mice and then differentiated in the presence of anti-CD3, anti-CD28, IL-2 and TGF-β1 in the absence or presence of AEP inhibitor for 3 days followed by expansion in IL-2 alone for another four days. At day 7, Foxp3 expression was measured by intracellular flow cytometry (**C**). Summary of Foxp3 expression in the various cohorts was shown (**D**). Tbet⁺iTreg^{PDL1} cells were activated with anti-CD3, anti-CD28, IL-2 and TGF-β1 for 24 hrs and then transduced with human AEP RV. At day 4, cell lysates were measured for human AEP protein expression (**E**). Transduced cells were stained with DAPI and AEP LE28 Cy5 probe and then subjected to confocal microscopy (**F**). *Aep*^{-/-} iTreg cells were transduced with empty vector or AEP over-expressing RV and then Foxp3 stability was tested at day 7 post expansion (**G**). Tbet⁺iTreg cells from WT mice were activated with anti-CD3, anti-CD28, IL-2 and TGF-β1 for 24 hrs and then transduced with mouse control (scramble) shRNA or AEP shRNA. At day 4, AEP expression was measured by immunoblot analysis (**H**), expression of Thy1.1 in the transduced cells (**I**), and active AEP was measured by flow cytometry (**J**). AEP was mutated at the nuclear localization sequence and then cloned into a Thy1.1 vector. CD4⁺CD25⁻ T cells were isolated from *Aep*^{-/-} mice and then stimulated under iTreg conditions. During the stimulation, cells were infected with retrovirus containing either empty vector (EV), AEP overexpressing vector (AEP RV) or AEP NLSmu (KRK-AAA mutation, site 318-320). Successful infection was measured by flow cytometry in the various cohorts using the AEP Cy5 probe (**K**). At day 7, Foxp3 expression was measured by flow cytometry in the listed cohorts (**L-M**). Experiments were repeated three times and data shown are Mean±SEM.

Supplementary Figure 6 (related to Figure 5)

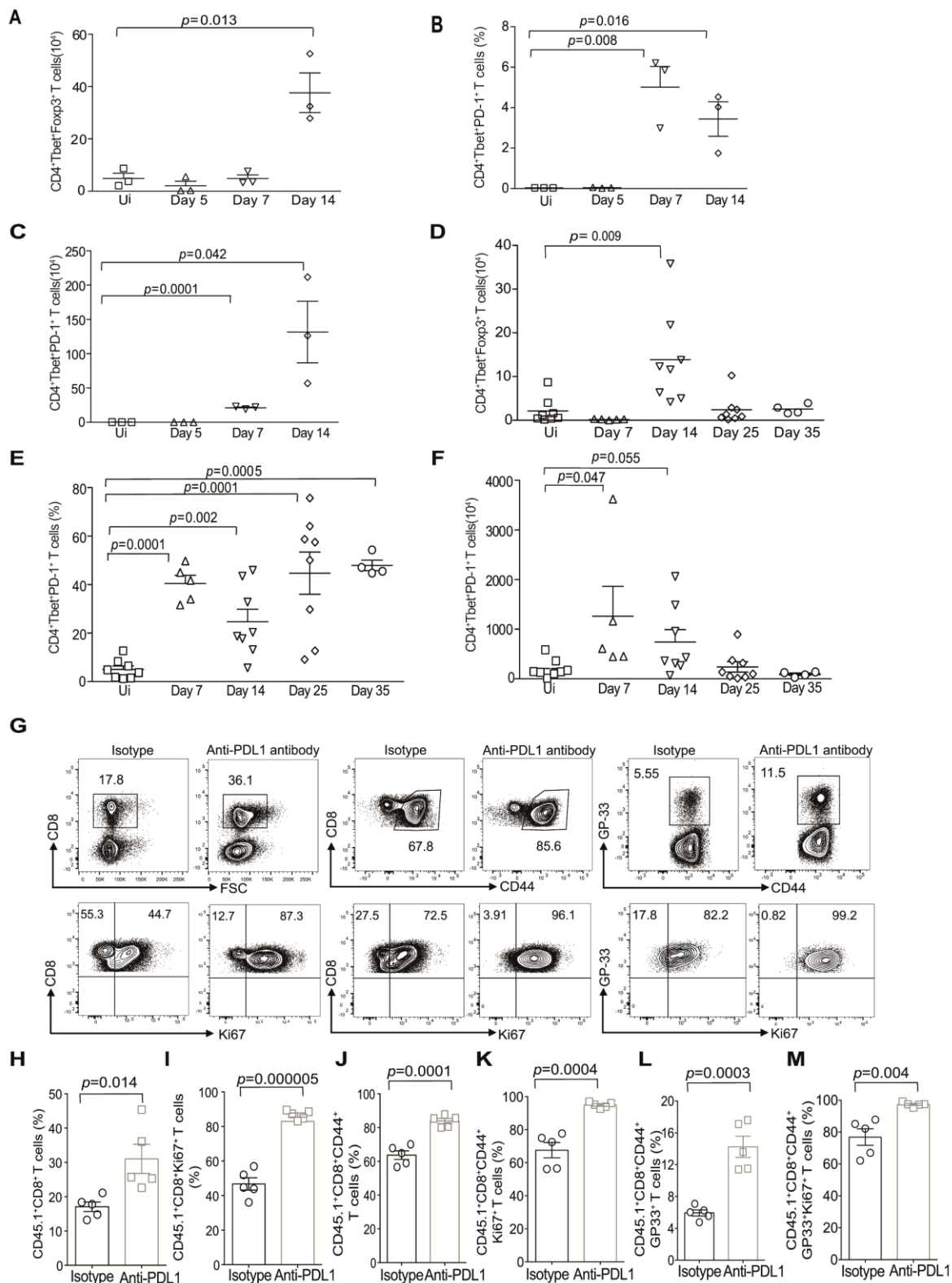


AEP deficiency delays loss of Foxp3 *in vivo*

Splenocytes were harvested from WT and *Aep*^{-/-} mice, and then CD4⁺Foxp3⁺ T cells were characterized for Treg markers namely CD25, CD127, Neuropilin-1 and Helios (A-B). Splenocytes were stimulated for 4 hrs in the presence of PMA plus ionomycin and then treated with golgiplug and golgistop for the last 2 hrs of stimulation. Cells were then stained for Th1 cell, Th2 cell, Th17 cell

specific cytokines and subjected to intracellular cytometry (C). Naïve T cells from WT and *Aep*^{-/-} mice were isolated, differentiated under iTreg conditions for 3 days. Foxp3 expression was analyzed in *in vitro* induced WT and *Aep*^{-/-} Treg cells (D). Balb/c mice were subjected to total body irradiation, followed by reconstitution with CD45.1⁺ bone marrow cells plus CD45.1⁺CD4⁺CD25⁻ T cells. Certain cohorts received CD45.2⁺ WT or *Aep*^{-/-} iTreg cells in addition to bone marrow cells and CD45.1⁺CD4⁺CD25⁻ T cells. Foxp3 expression within the WT and *Aep*^{-/-} iTreg cells at day 14 post-transplant (E). Frequency of CD45.2⁺Foxp3⁺ cells in the spleen and lymph nodes of the various cohorts (F). Experiments were repeated twice and each cohort had n=4-5 mice. Data are shown as Mean±SEM.

Supplementary Figure 7 (related to Figure 6)



Tbet^{hi} cells express PD-1 during acute and chronic LCMV infection

B6.*Tbx21*Zsgreen*Foxp3*RFP mice were infected with LCMV Armstrong (2×10^5 PFU) and then monitored for CD4⁺Tbet^{hi}FoxP3⁺ cells and CD4⁺Tbet^{hi}PD-1⁺ cell kinetics. Absolute numbers of CD4⁺Tbet^{hi}FoxP3⁺ cells (A), frequency of PD-1 expressing cells at different time points (B), and absolute numbers of PD-1 expressing cells at different time points were shown (C).

B6.*Tbx21*ZsGreenFoxp3RFP mice were infected with LCMV Clone-13 (2×10^6 PFU) and then monitored for CD4⁺Tbet^{hi}FoxP3⁺ cells and CD4⁺Tbet^{hi}PD-1⁺ cells kinetics. Absolute numbers of CD4⁺Tbet^{hi}FoxP3⁺ cells (**D**), frequency of PD-1 expressing cells at different time points (**E**), and absolute numbers of PD-1 expressing cells at different time points were shown (**F**). CD45.1⁺ hosts were infected with Clone 13 and reconstituted with CD45.2⁺CD4⁺Tbet⁺FoxP3⁻ cells. Cohorts were treated with isotype or anti-PDL1 antibody (200 μ g/mouse). At day 10, splenocytes were harvested and the frequency of CD45.1⁺CD8⁺ T cells (**G**, left two top panels; **H**), that were Ki67⁺ (**G**, left two bottom panels; **I**) were determined. The frequency of CD8⁺CD44⁺ cells (**G**, top middle panels; **J**), that were Ki67⁺ cells (**G**, bottom middle panels; **K**) is shown. The frequency of GP33 specific CD8⁺ T cells (**G**, top right two panels; **L**), and that were Ki67⁺ (**G**, bottom right two panels; **M**) were measured. Experiments were repeated twice and each cohort had n=3-8 mice. Representative data from one experiment is shown as Mean \pm SEM.

Supplementary Table 1: AEP-specific semi-tryptic cleavage in Foxp3 bands 2 and band 3 (related to Figure 3)

Sequence-Band 2- AEP cleavage site	Start	Stop
(R)PGKPSAPSLALGPSPGASPSWR(A)	6	27
(K)ASDLLGAR(G)	32	39
(N)VASLEWVSR(E)	155	163
(R)KDSTLSAVPQSSYPLLANGVcK(W)	179	200
(K)VFEEDDFLK(H)	207	216
(R)EmVQSLEQQLVLEK(E)	237	250
(R)EMVQSLEQQLVLEK(E)	237	250
(R)EmVQSLEQQLVLEK(E)	237	250
(L)SAmQAHLAGK(M)	254	263
(K)GSccIVAAGSQGPVPAWSGPR(E)	278	299
(R)EAPDSLFAVRR(H)	300	310
(R)WAILEAPEK(Q)	348	356
(R)WAILEAPEKQR(T)	348	358
(K)cFVRVESEK(G)	394	402
(K)GAVWTVDELEFRK(K)	403	415
Sequence-Band 3- Additional degraded band		
(R)PGKPSAPSLALGPSPGASPSWR(A)	6	27
(K)ASDLLGAR(G)	32	39
(R)GPGGTFQGR(D)	40	48
(R)GGAHASSSSLNPmPPSQLQLPTLPLVmVAPSGAR(L)	52	85
(R)KDSTLSAVPQSSYPLLANGVcK(W)	179	200
(R)EmVQSLEQQLVLEK(E)	237	250
(R)EMVQSLEQQLVLEK(E)	237	250
(R)EmVQSLEQQLVLEK(E)	237	250
(R)EMVQSLEQQLVLEKEK(L)	237	252
(L)SAmQAHLAGK(M)	254	263
(R)WAILEAPEK(Q)	348	356